Global and Planetary Change 182 (2019) 103005

Contents lists available at ScienceDirect

Global and Planetary Change

journal homepage: www.elsevier.com/locate/gloplacha

Research article

# Future projections of cyclone activity in the Arctic for the 21st century from regional climate models (Arctic-CORDEX)

Mirseid Akperov[a,*], Annette Rinke[b], Igor I. Mokhov[a,c], Vladimir A. Semenov[a,d], Mariya R. Parfenova[a], Heidrun Matthes[b], Muralidhar Adakudlu[e], Fredrik Boberg[n], Jens H. Christensen[e,f,n], Mariya A. Dembitskaya[a], Klaus Dethloff[b], Xavier Fettweis[g], Oliver Gutjahr[h], Günther Heinemann[i], Torben Koenigk[j,q], Nikolay V. Koldunov[k,l], René Laprise[m], Ruth Mottram[n], Oumarou Nikiéma[m], Dmitry Sein[l,r], Stefan Sobolowski[e], Katja Winger[m], Wenxin Zhang[o,p]

[a] A.M. Obukhov Institute of Atmospheric Physics, RAS, Moscow, Russia
[b] Alfred Wegener Institute, Helmholtz Centre for Polar and Marine Research, AWI, Potsdam, Germany
[c] Lomonosov Moscow State University, Moscow, Russia
[d] Institute of Geography, RAS, Moscow, Russia
[e] NORCE Norwegian Research Centre, Bjerknes Centre for Climate Research, Bergen, Norway
[f] University of Copenhagen, Niels Bohr Institute, Denmark
[g] Department of Geography, University of Liège, Belgium
[h] Max Planck Institute for Meteorology, Hamburg, Germany
[i] Environmental Meteorology, Faculty of Regional and Environmental Sciences, University of Trier, Germany
[j] Rossby Centre, Swedish Meteorological and Hydrological Institute, 60176 Norrköping, Sweden
[k] MARUM - Center for Marine Environmental Sciences, Bremen, Germany
[l] Alfred Wegener Institute, Helmholtz Centre for Polar and Marine Research, AWI, Bremerhaven, Germany
[m] Centre ESCER, Université du Québec à Montréal, Montréal, Québec, Canada
[n] Danish Meteorological Institute, Copenhagen, Denmark
[o] Department of Physical Geography and Ecosystem Science, Lund University, 22362, Lund, Sweden
[p] Center for Permafrost (CENPERM), Department of Geosciences and Natural Resource Management, University of Copenhagen, Copenhagen, Denmark
[q] Bolin Centre for Climate Research, Stockholm University, 10654 Stockholm, Sweden
[r] Shirshov Institute of Oceanology, RAS, Moscow, Russia

ARTICLE INFO

*Keywords:*
Arctic
Cyclone activity
Climate change
Regional climate models
CMIP5 models
CORDEX

ABSTRACT

Changes in the characteristics of cyclone activity (frequency, depth and size) in the Arctic are analyzed based on simulations with state-of-the-art regional climate models (RCMs) from the Arctic-CORDEX initiative and global climate models (GCMs) from CMIP5 under the Representative Concentration Pathway (RCP) 8.5 scenario. Most of RCMs show an increase of cyclone frequency in winter (DJF) and a decrease in summer (JJA) to the end of the 21st century. However, in one half of the RCMs, cyclones become weaker and substantially smaller in winter and deeper and larger in summer. RCMs as well as GCMs show an increase of cyclone frequency over the Baffin Bay, Barents Sea, north of Greenland, Canadian Archipelago, and a decrease over the Nordic Seas, Kara and Beaufort Seas and over the sub-arctic continental regions in winter. In summer, the models simulate an increase of cyclone frequency over the Central Arctic and Greenland Sea and a decrease over the Norwegian and Kara Seas by the end of the 21st century. The decrease is also found over the high-latitude continental areas, in particular, over east Siberia and Alaska. The sensitivity of the RCMs' projections to the boundary conditions and model physics is estimated. In general, different lateral boundary conditions from the GCMs have larger effects on the simulated RCM projections than the differences in RCMs' setup and/or physics.

* Corresponding author.
*E-mail address:* aseid@ifaran.ru (M. Akperov).

https://doi.org/10.1016/j.gloplacha.2019.103005
Received 8 April 2019; Received in revised form 11 August 2019; Accepted 14 August 2019
Available online 17 August 2019

## 1. Introduction

The Arctic warming in recent decades has been proceeding at least two times faster than the global temperature increase and is accompanied by an unprecedented reduction of sea ice extent, and these changes affect large scale atmospheric circulation and weather patterns in high- and mid-latitudes (e.g. Vihma, 2014; Semenov and Latif, 2015). The Arctic Ocean has become more accessible for marine shipping along the Northern Sea Route (Khon et al., 2017), extraction of oil and natural gas resources and other activities such as tourism or fishing. However, all these activities are affected by weather conditions, in particular, cyclone activity.

Cyclones play an important role in the coupled dynamics of the Arctic climate system, in particular, they are contributing to the meridional transport of atmospheric heat and moisture from mid-latitudes, thereby changing wind, temperature, precipitation and sea ice distribution in the Arctic (e.g. Alexeev et al., 2017). The influence of a changing climate on cyclone activity characteristics is complicated as the response is dependent on many dynamical and thermodynamical processes (e.g. Mokhov et al., 1992; Inoue et al., 2012; Akperov and Mokhov, 2013). Therefore, understanding changes in storminess in the Arctic region is important to properly manage the risks associated with these events in a changing climate system.

One of the powerful tools to assess the impacts of climate change on cyclone activity are global climate models (GCMs), which are widely used to analyze midlatitude cyclones (e.g. Ulbrich et al., 2013). However, the results for the response of the Arctic cyclones to climate change from GCM studies show some disagreement. One of the reasons may be related to inter-model variability of cyclone activity characteristics across the GCMs in midlatitudes (Zappa et al., 2013).

Using an ensemble of CMIP3 models under SRES-A1B scenario, Lang and Waugh (2011) found a significant decrease in the number of cyclones in the Norwegian Sea and an increase over the Barents Sea, Baffin Bay, Davis Strait, and near the southern tip of Greenland in winter, and no significant changes in summer by 2100. They also noted a large decrease in the number of intense winter cyclones over the Arctic Ocean. Changes of cyclone activity in the 21st century from simulations with the ECHAM5/MPI–OM GCM under SRES-A1B scenario were analyzed by Ulbrich et al. (2013) using different methods of cyclone identification. They also found a decrease of cyclone numbers in the Barents and Greenland Seas for the winter in the second half of the 21st century. Orsolini and Sorteberg (2009) found an increase in the number of cyclones entering the Arctic in the summer as well as for the mean intensity by the end of the 21st century using BCM v2.0 GCM under SRES-A1B and SRES-A2 scenarios. They also noted that the cyclone increase is associated with an increase in zonal wind and meridional temperature gradient at high latitudes in summer, due to the slower Arctic Ocean warming compared to the surrounding land. Using an ensemble of CMIP3 as well as CMIP5 simulations, Nishii et al. (2015) found an increase in Arctic summer storminess across these ensembles. They found, in agreement with Orsolini and Sorteberg (2009), that the magnitude of the response of cyclone activity was strongly correlated with the magnitude of change in the zonal mean wind and the surface air temperature gradient along the Eurasian coastline.

Using CMIP5 models under various Radiative Concentration Pathway (RCP) scenarios, Colle et al. (2013) found a reduction of cyclone number over the western Atlantic and an increase near Nova Scotia in southeast Canada in cold season. Zappa et al. (2013) noted that the number and the wind intensity of cyclones decreases in the Norwegian Sea in the cold season and increases near the southern tip of Greenland in the warm season. Harvey et al. (2015) also found reductions in Arctic winter storminess at the end of the 21st century. Day and Hodges (2018) investigated the response of Arctic cyclones to climate change in a large initial value ensemble of future climate projections with the CESM1-CAM5 (CESM-LE). They found a significant reduction in cyclone frequency in winter and insignificant changes in summer. It has been also noted a reduction of cyclone intensity across the Arctic basin in winter, but with contrasting increase in summer intensity within the Arctic Ocean cyclone maximum. The study also showed a significant reduction in winter cyclogenesis events within the Greenland–Iceland–Norwegian Sea region. They emphasized that the seasonal response of cyclone intensity and cyclogenesis appears to be closely linked to changes in surface temperature gradients in the high latitudes, with Arctic poleward temperature gradients increasing in summer, but decreasing in winter. Crawford and Serreze (2017) investigated the relationship between the Arctic frontal zone and summer Arctic cyclone activity for the RCP8.5 scenario using the same CESM-LE ensemble. They showed a decrease of cyclones in the Barents, Kara, and Laptev Seas and an increase along the eastern side of Greenland and Chukchi and Beaufort Seas in summer. Detailed information about the changes of cyclone frequency as a function of region, seasons, climate models, scenarios is presented in Supplementary Table 1.

In addition to using different models and scenarios, each of these studies uses different periods of analysis, and storm intensity/activity measures, all of which may influence the results. Also, the relative coarse resolution of the GCMs and deficits in the representation of physical processes in the Arctic cause uncertainties to the projections of future changes of cyclone activity. The interest in better representing the climate variability and change at regional scales has driven the development of regional climate models (RCMs). RCMs run on limited area domains thereby allowing increased spatial resolution, and thus enabling a better representation of mesoscale atmospheric processes, which are important for cyclone activity. The international CORDEX (Coordinated Regional Climate Downscaling Experiment) (Giorgi et al., 2009) has provided multi-model RCM simulations at high spatial resolution over different regions in the world. As a part of the CORDEX framework, the Arctic-CORDEX initiative (http://www.climate-cryosphere.org/activities/targeted/polar-cordex/arctic) provides RCM projections for the Arctic at ca. 50 km (ARC-44) resolution.

Several studies demonstrated the usefulness of RCMs for studying extratropical cyclones (Côté et al., 2015) and Arctic cyclones (Shkolnik and Efimov, 2013; Akperov et al., 2015; Akperov et al., 2018). Recently, Akperov et al. (2018) showed that the state-of-the-art RCMs from Arctic-CORDEX are able to simulate realistically the present-day cyclone activity characteristics in the Arctic compared to reanalysis data.

The general aim of this paper is to analyze possible future changes of cyclone characteristics (frequency, depth, and size) over the Arctic region using a multi-model ensemble of RCM simulations (Arctic-CORDEX) for the 21st century. We further address how different GCM as lateral boundary conditions affect the RCMs results.

## 2. Data and methods

### 2.1. Model and reanalyses data

We analyze cyclone characteristics obtained from 6-hourly mean sea level pressure (MSLP) data from an ensemble of six atmospheric RCMs (CRCM5, HIRHAM5-AWI, HIRHAM5-DMI, MAR3.6, RCA4, RCA4-GUESS), four GCMs (NorESM1, CanESM2, MPI-ESM-LR, EC-EARTH) and four reanalysis products (ERA-Interim, NCEP-CFSR, NASA-MERRA2, JMA-JRA55) (Table 1) for the Arctic region (north of 65°N) for two seasons – winter (DJF) and summer (JJA).

The six Arctic-CORDEX RCMs (Table 1) are based on the standard Arctic CORDEX model setup (http://climate-cryosphere.org/activities/targeted/polar-cordex/arctic). All RCMs are atmospheric RCMs, but in one of the models (RCA-GUESS) the land surface scheme is interactively coupled with the vegetation-ecosystem model LPJ-GUESS (Smith et al., 2011; Zhang et al., 2014). More detailed information about the RCMs is presented in Table 1. The RCMs apply the Arctic CORDEX grid (rotated 0.44° × 0.44° grid, 116 × 133 grid points), and all other data (GCMs and reanalyses) have been bilinearly interpolated onto that grid for

**Table 1**
Reanalyses, global climate models (GCMs) and regional climate models (RCMs), and their corresponding information.

| Type | Institution/country | Data/model name | Original Resolution Vertical, horizontal | Boundary conditions | Reference |
|---|---|---|---|---|---|
| Reanalyses | ECMWF/UK | ERA-Interim | L60, 0.75$^0$ (~ 83 km) | | Dee et al. (2011) |
| | NASA/USA | MERRA2 | L72, 0.5$^0$ × 0. 625$^0$ (~56 km) | | Gelaro et al. (2017) |
| | NCEP/USA | CFSR | L64, 0.5$^0$ (~56 km) | | Saha et al. (2010) |
| | JMA/JAPAN | JRA55 | L60, 0.5$^0$ (~ 56 km) | | Ebita et al. (2011); Kobayashi et al. (2015); |
| Regional climate models (RCMs) | AWI/Germany | HIRHAM5-AWI-MPI<br>HIRHAM5-AWI-EC-EARTH | L40, 0.5$^0$ (~56 km) | MPI-ESM-LR<br>EC-EARTH | Christensen et al. (2007); Sommerfeld et al. (2015); Klaus et al. (2016) |
| | DMI/Denmark | HIRHAM5-DMI-EC-EARTH | L31, 0.44$^0$ (~48 km) | EC-EARTH | Christensen et al. (2007); Lucas-Picher et al. (2012) |
| | SMHI/Sweden | RCA4 -MPI<br>RCA4-EC-EARTH<br>RCA4-CanESM2<br>RCA4-NorESM1 | L40, 0.44$^0$, (~48 km) | MPI-ESM-LR<br>EC-EARTH<br>CanESM2<br>NorESM1-M | Berg et al. (2013); Koenigk et al. (2015) |
| | LU/Sweden | RCA-GUESS-EC-EARTH | L40, 0.44$^0$, (~48 km) | EC-EARTH | Smith et al. (2011); Zhang et al. (2014) |
| | ULg/Belgium | MAR3.6-NorESM1 | L23, 50 km (~0.5$^0$) | NorESM1-M | Fettweis et al. (2017) |
| | UQAM/Canada | CRCM5-MPI<br>CRCM5-MPIC<br>CRCM5- CanESM2 | L55, 0.44$^0$, (~48 km) | MPI-ESM-LR<br>MPI-ESM-LR (Bias correction)<br>CanESM2 | Martynov et al. (2013); Šeparović et al. (2013); Takhsha et al. (2017) |
| Global climate models (GCMs) | MPI/Germany | MPI-ESM-LR | L47, 1.8$^0$ (~200 km) | | Giorgetta et al. (2013) |
| | ICHEC/EU | EC-EARTH | L62, 1.1$^0$ (~122 km) | | Hazeleger et al. (2012) |
| | CCCma/Canada | CanESM2 | L35, 2.8$^0$ (~310 km) | | Arora et al. (2011) |
| | NCC/Norway | NorESM1-M | L26, 2.5$^0$ (~277 km) | | Bentsen et al. (2013) |

better comparison.

The RCM simulations are driven by the four above-mentioned CMIP5 GCMs for a historical period (from 1950 to 2005) and for a future period (from 2006 to 2099) for the RCP8.5 (Taylor et al., 2012) (Table 1). We focus our analysis of future cyclone changes on the 30-year periods 1970–1999 as historical (reference) period and 2070–2099 as future period. For comparing the RCM results with the reanalyses for present-day, we use the period 1980–2005.

In summary, we analyze a set of 12 RCM simulations from six different RCMs, which have been driven by four different GCMs. See Table 1 for more details about the RCM-GCM matrix.

This ensemble includes an experiment in which the GCM-simulated sea surface temperature (SST) is empirically corrected and used as lower boundary conditions for an atmosphere-only global simulation (AGCM), which in turn provides the atmospheric boundary conditions to drive the CRCM5 simulation (Takhsha et al., 2017).

### 2.2. Cyclone identification

We use an algorithm of cyclone identification similar to Bardin and Polonsky (2005) and Akperov et al. (2007) with some modifications for the Arctic region (Akperov et al., 2015). The algorithm is based on the MSLP field and has been shown to be useful to investigate the changes in cyclone activity in extratropical and high latitudes (Akperov and Mokhov, 2010; Neu et al., 2013; Ulbrich et al., 2013; Simmonds and Rudeva, 2014; Akperov et al., 2015). We calculate cyclone frequency, depth and size. The cyclone frequency is defined as the number of cyclone events per season. We consider the cyclone depth as a measure of cyclone intensity. The cyclone depth is determined as the difference between the minimum central pressure in the cyclone and the outermost closed isobar. As shown in previous studies (Golitsyn et al., 2007; Simmonds and Keay, 2009), the depth provides a direct measure of the kinetic energy of the system. The cyclone size (radius) is determined as the average distance from the geometric center to the outermost closed isobar. The details of this algorithm and its application for detection of the variability and changes in cyclone activity over the Arctic are discussed in previous studies (Akperov et al., 2015; Akperov et al., 2018; Zahn et al., 2018). To map spatial patterns of cyclone characteristics we use the grid with circular cells of a 2.5° latitude radius. Cyclones over regions with surface elevations higher than 1000 m are excluded due to larger uncertainty in the MSLP fields resulted from the extrapolation to the sea level.

The spatial correlation analysis is based on the Pearson correlation coefficient (R). As an indicator of the robustness of cyclone characteristics changes we calculate their statistical significance using a Student's *t*-test at the 90% confidence level ($P < .1$).

## 3. Cyclone characteristics from RCMs in present-day climate

Here we analyze the historical simulations (hist), performed using 6 RCMs driven by 4 different GCM at the boundaries (see Table 1). Cyclone activity obtained from these RCMs is compared to the multi-reanalyses mean for the overlapping period of 1980–2005. The aim is to demonstrate the realistic simulation of cyclone characteristics by the Arctic-CORDEX RCMs for the historical period.

### 3.1. Cyclone frequency

Fig. 1 displays the climatology of cyclone frequency for winter (DJF) and summer (JJA) from multi-reanalyses and the multi-model (RCM) means. The spatial patterns of cyclone frequency are well reproduced in the Arctic by the multi-model mean compared to the multi-reanalysis

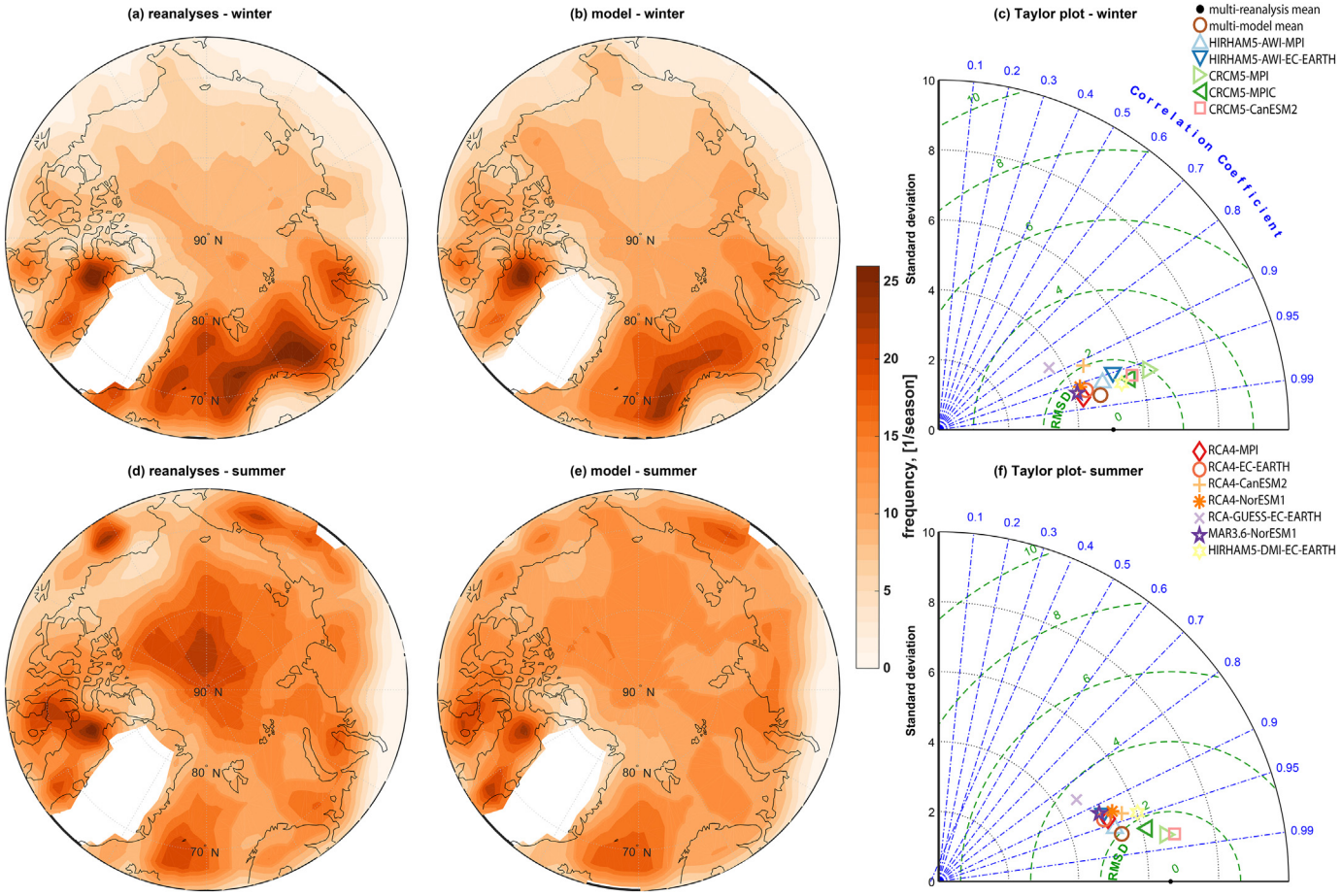


**Fig. 1.** Spatial distribution of cyclone frequency in winter (a,b) and summer (d,e) from multi-reanalyses mean and multi-model (RCM) ensemble mean for the period 1980–2005. Taylor plots of cyclone frequency of RCMs and reanalysis data for winter (c) and summer (f). Reference for Taylor plot is the multi-reanalyses mean. Cyclones over regions with surface elevations higher than 1000 m are masked out.

data for both seasons. Maxima of cyclone frequency in winter is located over the Baffin Bay, Davis Strait, southeast of Greenland and over the Nordic Seas. Compared to winter, the cyclone frequency in summer is higher over land, in particular over Eastern Siberia, Chukotka, Alaska and also over the central Arctic. Wherein the general low cyclone frequency over the Arctic Ocean in the models may be explained by low baroclinicity and weak polar front jet over Eurasia (e.g. Lee, 2014). These seasonal cyclone frequency patterns agree with previous studies (e.g., Wernli and Schwierz, 2006; Simmonds et al., 2008; Akperov et al., 2018).

The spatial correlation coefficients (R) between the individual models and multi-reanalysis mean cyclone frequency range from 0.87 (RCA-GUESS-EC-EARTH) to 0.97 (RCA4-MPI) in winter and from 0.85 (RCA-GUESS-EC-EARTH) to 0.98 (CRCM5-CanESM2) in summer (Fig. 1c,f). The spatial standard deviations (STD) range from 3.6 (4.6) to 6.2 (6.9) cyclones per season in winter (summer). Respective root mean square errors (RMSE) vary from 1.3 (1.2) to 2.6 (3.6) cyclones per season for winter (summer). The spatial correlation coefficients between the multi-model mean and the multi-reanalyses mean for winter (summer) are 0.98 (0.97), with STDs of 4.7 (5.4) cyclones per season, and RMSEs of 1.1 (1.9) cyclones per season, respectively.

Seven out of 12 RCM simulations show a lower cyclone frequency (relative to the multi-reanalyses mean) for the Arctic by up to 20% (RCA-GUESS-EC-EARTH) in winter (Fig. 2). In summer, nine models show this underestimation as well. Most models show less frequent occurrence of deep cyclones in both seasons (not shown). The underestimation ranges from −13% (CRCM5-CanESM2) to −61% (RCA4-CanESM2) in winter and from −1% (CRCM5-MPI) to −64% (MAR3.6-NorESM1) in summer. The differences across the four reanalyses are much smaller compared to the across-model differences.

The seasonal cycle for cyclone frequency is well captured by all models with higher cyclone frequency in summer and low frequency in winter (Supplementary Fig. 1). However, the models show a higher intra-ensemble variability of the monthly mean cyclone frequency compared to the reanalysis differences. Further, the models underestimate cyclone frequency in May, June, July and September.

### 3.2. Cyclone mean depth and size

The models reproduce the observed frequency distributions of cyclone size and depth (Supplementary Fig. 2). The multi-model mean also reproduces the spatial pattern of cyclone mean depth and size when compared to the results from multi-reanalyses data for both seasons (Supplementary Figs. 3 and 4). The deepest cyclones are located in the region between Greenland and the Barents Sea in winter and over the central Arctic Ocean in summer. The cyclones with largest radii are found over the central Arctic Ocean for both seasons. This agrees with previous findings for the climatological mean depth and size for the Arctic using reanalyses and model simulations (e.g. Simmonds et al., 2008; Shkolnik and Efimov, 2013; Akperov et al., 2015; Akperov et al., 2018; Zahn et al., 2018).

All individual models show high spatial correlation of cyclone mean depth for both seasons in comparison with the multi-reanalyses mean; the correlation coefficients vary from 0.89 (RCAGUESS-EC-EARTH) to 0.98 (CRCM5-CanESM2) in winter and from 0.94 (RCAGUESS-EC-EARTH) to 0.99 (CRCM5-MPI) in summer, respectively (Supplementary

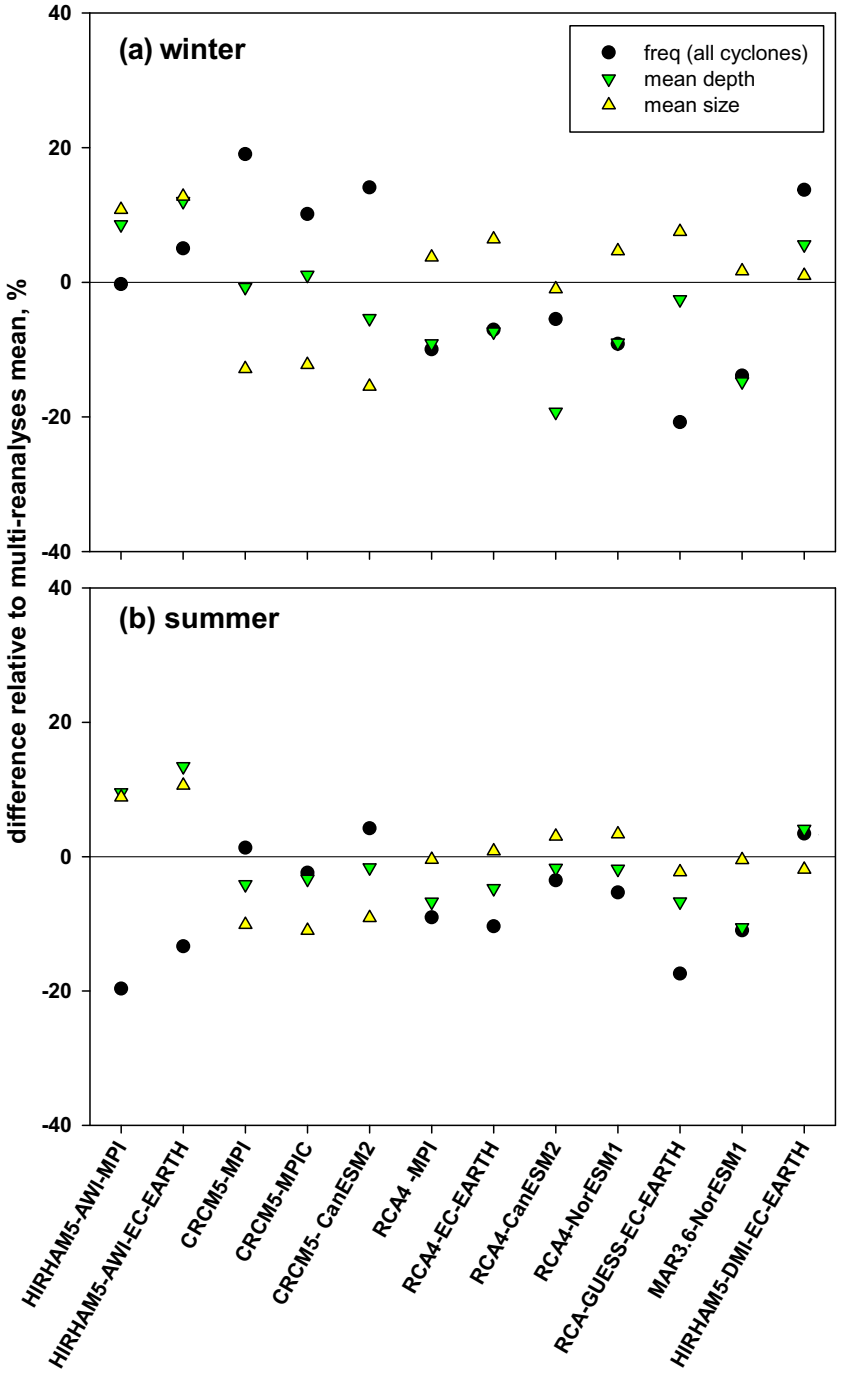


**Fig. 2.** Relative biases of RCM simulated cyclone characteristics (relative to the multi-reanalysis mean), black dot – cyclones frequency, green triangle – cyclone mean depth, yellow triangle - cyclone mean size in winter (a) and summer (b) for the period 1980–2005. (For interpretation of the references to colour in this figure legend, the reader is referred to the web version of this article.)

Fig. 3 c,f). Standard deviations vary between 3.1 (2.7) and 4.6 (3.6) hPa for winter (summer) and corresponding RMSEs vary from 0.7 (0.4) to 1.8 (1.2) hPa. The spatial correlation coefficients for the multi-model mean for summer are slightly higher than the coefficient for winter, with $R = 0.97$ (0.98), and with STD = 3.8 (3.1) hPa and RMSE = 0.8 (0.6) hPa for winter (summer). Most Arctic CORDEX models show smaller cyclone mean depth when compared with the multi-reanalyses mean for both seasons (Fig. 2). This underestimation varies from −19% (RCA4-CanESM2) to −1% (CRCM5-MPI) in winter and from −11% (MAR3.6-NorESM1) to −2% (CRCM5-CanESM2) in summer. This underestimation may be related to too weak zonal wind speeds, which leads to an underestimation of cyclone mean depth and deep cyclone frequency in the Arctic (Akperov et al., 2018).

The spatial correlation for cyclone mean size between Arctic CORDEX model mean and the multi-reanalyses mean is also high (larger than 0.99 for both seasons) (Supplementary Fig. 4). The RMSEs vary from 31 (28) km to 53 (47) km and STDs vary from 194 (219) km to 258 (268) km for winter (summer). The spatial correlation coefficients between the multi-model mean and the multi-reanalyses mean for both seasons are high (0.98) with STD of 230 (240) km and RMSE of 33 (38) km for winter (summer). Most models consistently simulate larger (smaller) sized cyclones in winter (summer) compared to the

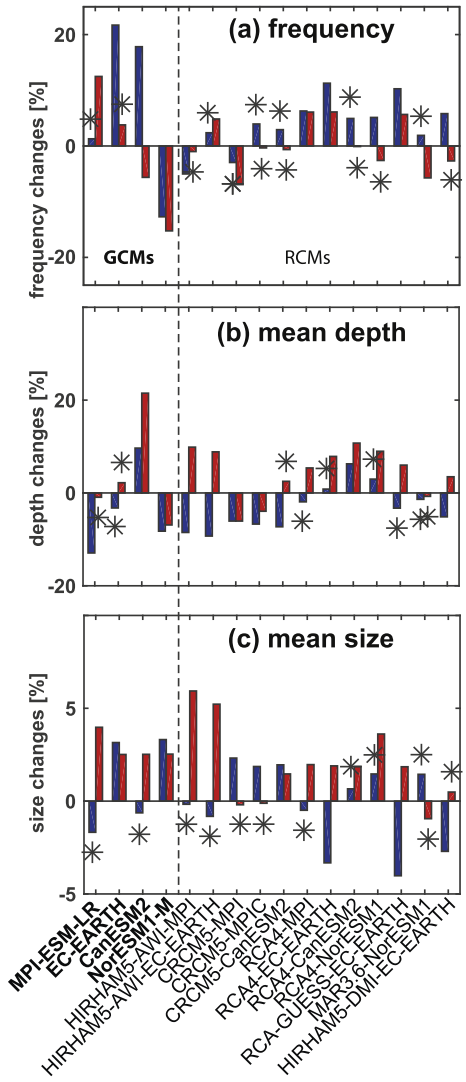


**Fig. 3.** Changes of cyclone characteristics ("RCP8.5" – "hist") (%) for cyclone frequeny (a), cyclone mean depth (b), and size (c) from RCMs and GCMs in winter (blue) and summer (red), averaged over the Arctic. The vertical line separates global and regional models. Black asterisks show statistical significance ($p < .1$). GCMs are highlighted in bold. (For interpretation of the references to colour in this figure legend, the reader is referred to the web version of this article.)

multi-reanalyses mean (Fig. 2). Eight out of 12 RCMs overestimate cyclone mean size by up to +12% (HIRHAM5-AWI-EC-EARTH) in winter. In summer, seven models show too small cyclone mean size, which varies from −1% (RCA4-MPI) to −11% (CRCM5-MPIC). Differences in mean size between RCMs and multi-reanalyses mean may be explained by a different representation of the vertical and horizontal temperature distribution in the models, which change the stability in the atmosphere and thus the cyclone characteristics in the Arctic. For instance, the Rossby radius (cyclone size) depends only on the vertical stratification of the temperature (Brunt-Väisälä frequency).

## 4. Changes of cyclone characteristics by the end of the 21st century

The analysis of changes in cyclone characteristics in the Arctic in the last three decades of the 21st century (2070–2099) simulated by RCMs under the RCP8.5 scenario relative to the historical (1970–1999) period is presented here (Fig. 3). We also compare RCM results with those from the driving GCMs.

We define a climate change signal to be robust if the following two conditions are fulfilled: > 75% of model simulations agree on the sign of the change and the signal to noise ratio (SNR), i.e. the ratio of the mean to the standard deviation of the ensemble of climate change signals, is equal to or larger than one. The second criterion is a measure of the strength of the climate change signal (with respect to the inter-model variability in that signal). We use the second criterion in addition to the first, because the first criterion alone may be not sufficient as it may be fulfilled even in the case of a very small, close to zero change (Mba et al., 2018; Nikulin et al., 2018).

Most RCMs (9 out of 12) and most GCMs (3 out of 4) simulate an increase of cyclone frequency, averaged over the Arctic in winter. In summer, 7 out of 12 RCMs show a decrease while the GCMs show different tendencies: two models (MPI-ESM-LR and EC-EARTH) show positive changes, the other two (CanESM2 and NorESM1) exhibit negative changes (Fig. 3). For the cyclone mean depth changes, 9 out of 12 RCMs and 3 out of 4 GCMs agree on a decrease in winter. In contrast, in summer, an increase of cyclone depth is obvious in most RCMs (9 out of 12). The sign of change is, however, less robust in the GCMs, where two models (EC-EARTH and CanESM2) show an increase of cyclone depth and the other two models (MPI-ESM-LR and NorESM1) show a decrease. For cyclone size changes in winter, only half of the RCMs display a similar behavior as compared to the depth changes, i.e., only six models show a decrease and the other six models show an increase. The same changes are obtained from GCMs: MPI-ESM-LR and CanESM2 simulate a decrease while the other two models show an increase in cyclone mean size in winter. In summer, most RCMs (9 out of 12) and all GCMs show an increase of cyclone mean size.

Fig. 4 illustrates the agreement among the RCMs and GCMs in the simulated changes of the spatial patterns of cyclone frequency for both seasons. Overall, the agreement in the spatial patterns is striking (pattern correlation between changes simulated by RCM and GCM is larger than 0.8) for all three cyclone characteristics in both seasons. Both RCMs and GCMs agree on the same changes in winter in the following regions: increased cyclone frequency over the Baffin Bay, Barents Sea, north of Greenland and Canadian Archipelago, and a decrease over the Nordic Seas, Kara and Beaufort Seas and the continents. The signal is robust for most regions in the GCMs and RCMs. Most RCMs simulate also a decrease over the East Siberian Sea, whereas all GCMs show an increase. Differences in changes of cyclone frequency between RCMs and GCMs are noted in winter over the Arctic Ocean, where most RCMs show an increase, while GCMs agree on a decrease. The reason of these discrepancies may be related to low cyclone frequency in GCMs due to low levels of baroclinicity and weak polar front jet over Eurasia in the models, which can affect these changes.

In summer, the models agree on an increase over the Greenland Sea and on a decrease over the Norwegian and Kara Seas and over the continents, in particular, over east Siberia and Alaska. Differences are also obvious for most parts of the Arctic Ocean, where most RCMs show positive changes, while most GCMs show negative changes.

Both RCMs and GCMs also largely agree on the patterns of changes in cyclone mean depth and size (Supplementary Figs. 5 and 6). The models simulate an increase of cyclone mean depth (intensity) over Siberia and Canadian Archipelago and a decrease over the Arctic Ocean, Barents Sea, Alaska and Davis Strait in winter. In summer, common areas of increase are located over the Beaufort, Chukchi, Barents and Greenland Seas and a decrease is found mostly over the sub-arctic continents. Very similar patterns are found for cyclone mean size.

## 5. Effects of boundary conditions (BCs) and RCM physics on cyclone characteristics under climate change

### 5.1. Same RCM with different BCs

Here we analyze runs from a certain RCM driven by various GCM

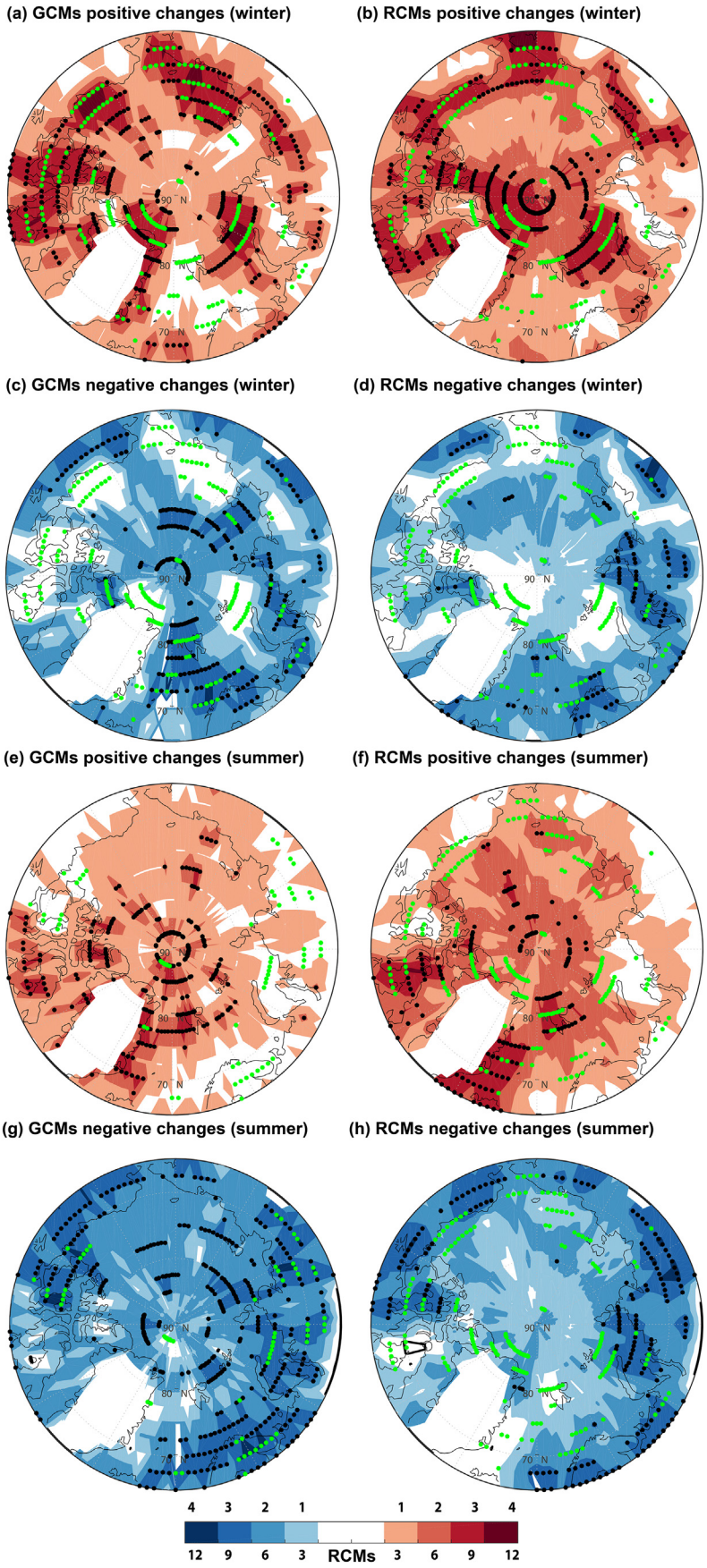


**Fig. 4.** Number of datasets showing positive or negative changes of cyclone frequency ("RCP8.5" – "hist") from GCMs (left column) and RCMs (right column) in winter (a, b, c, d) and summer (e, f, g, h). The colour scale represents the number of datasets with a positive (red colors) and negative (blue colors) changes. Cyclones over regions with surface elevations higher than 1000 m are masked out (see Fig. 1). Areas where at least 75% of the simulations (9 of 12 RCMs, 3 of 4 GCMs) agree on the sign of the change are marked by black dots. Areas where the signal to noise ratio (SNR) is equal or > 1 are marked by green dots. (For interpretation of the references to colour in this figure legend, the reader is referred to the web version of this article.)

forcing. By this, we aim to discuss the possible impact of the GCM forcing on the RCM projection. We have three RCMs (RCA4, HIRHAM5-AWI and CRCM5) which provide simulations with different boundary conditions (BCs) from different GCMs (Table 1). While HIRHAM5-AWI and CRCM5 have each been run with forcing from two different GCMs only, RCA4 has been run with four different GCMs (MPI-ESM-LR, EC-EARTH, CanESM2, NorESM1). Therefore, we present only a detailed analysis of the RCA4 projections.

First, we look at the Arctic mean changes in the cyclone frequency under RCP8.5 scenario obtained from the RCA4 model with different BCs (Fig. 3). The RCA4 runs show overall the same sign of change in cyclone frequency as the driving GCM does. This indicates the impact of the driving large-scale circulation on cyclone frequency in the RCM. However, the magnitude of change can be different. RCA4-MPI, RCA4-EC-EARTH and RCA-CanESM2 projections show positive changes, i.e. an increase of cyclone frequency in both seasons, in agreement with their driving GCM. RCA4-NorESM1 simulates a cyclone frequency increase (decrease) in winter (summer) which is partly in agreement with the driving NorESM1. For cyclone mean depth and size changes, the RCA4 projections mostly agree on the sign of the change with the driving GCMs, but show also some differences in both sign and magnitude. This indicates that cyclone depth and size changes are characteristics that depend stronger on the RCM physics than on the driving large-scale circulation. For cyclone size projections, RCA4 simulates an opposite change in winter compared to the driving GCM in two cases. RCA4-EC-EARTH simulates a strong decrease, whereas the driving GCM shows a strong increase. RCA4-CanESM2 simulates a small increase, but the driving GCM a small decrease. For cyclone mean depth, the major differences concern the RCA4-NorESM1, which simulates an increase in cyclone depth in winter and summer, which is opposite to the decrease seen in both seasons in the GCM.

If we look at the spatial distribution of the cyclone frequency changes, differences between the different RCA4 runs and driving GCM become obvious (Fig. 5). In general, the spatial correlations between RCA4-simulated cyclone characteristic changes and those from the driving GCM are moderate for both seasons (Table 2). This highlights regional differences in the spatial patterns. The agreement in cyclone frequency patterns across the RCA4 runs is larger in winter (spatial correlation across pairs of RCA4 simulations of 0.4–0.6) than in summer (spatial correlation across pairs of RCA4 simulations of 0.2–0.4) (Table 2, Fig. 5). In winter, RCA4 and GCMs agree on the significant increase of cyclone frequency in the Barents/Kara Sea, Baffin Bay, Arctic Ocean and in the Bering Strait region. In summer, the RCA4 patterns differ clearly from the patterns of their driving GCMs. This may indicate the dominant role of the large-scale forcing via the lateral BCs from the driving GCM for the regional downscaling in winter, whereas in summer, when the circulation is weaker, the role of the RCM physics becomes more prominent (e.g., Beniston et al., 2007; Christensen and Christensen, 2007). In summer, the large-scale circulation is also important, although the RCM (physics) itself has a large effect on cyclone characteristics due to diabatic and convective processes (e.g. Colmet-Daage et al., 2018).

### 5.2. Different RCMs with the same BCs

Here we analyze runs with different RCMs which have been driven by the same GCM. By this, we aim to discuss the impact of the RCM itself (e.g. its model physics) on the projections. According to the RCM-GCM matrix (Table 1), three RCMs (HIRHAM5-AWI, RCA4 and CRCM5) have been driven by the same BCs from MPI-ESM-LR, four RCMs (HIRHAM5-AWI, RCA4, RCA-GUESS and HIRHAM5-DMI) have been driven by the same BCs from EC-EARTH, two RCMs (CRCM5 and RCA4) have been driven by CanESM2, and another two RCMs (RCA4 and MAR3.6) have been driven by the same forcing of NorESM1. However, here we focus only on the EC-EARTH driven model runs, as this is the largest number of RCMs driven with this same BC.

Considering the whole Arctic, 3 out of 4 EC-EARTH-driven RCMs show an increase of cyclone frequency in both seasons, in agreement with the GCM (Fig. 3). However, none of them reproduces a similarly large increase of cyclone frequency as EC-EARTH in winter. Still, the results indicate a strong impact of the GCM large-scale dynamics on cyclone frequency changes. For cyclone mean depth and size changes, the across-RCM differences are larger, but still the models largely agree on the sign of change. Most RCMs simulate a decrease of cyclone mean depth and size in winter and an increase in summer.

Considering the spatial patterns of cyclone frequency changes, moderate agreement among the RCM simulations is found, particularly in winter (Figs. 5 and 6). An agreement in winter on cyclone frequency increase is found in the Chukchi Sea, Baffin Bay, Davis Strait, most parts of the Arctic Ocean, and northern Barents Sea and on cyclone frequency decrease in southern Kara Sea and northern Beaufort Sea. In summer, the areas of consistent changes are reduced relative to winter. An agreement on cyclone frequency increase is found mostly over the oceans, and on decrease over the continents (Fig. 5f, Fig. 6b,d,f).

The spatial correlation coefficients between these four RCMs are moderate in winter. They range from 0.3 (RCA-GUESS vs. HIRHAM5-DMI) to 0.6 (RCA4 vs. RCA-GUESS) in winter and from 0.1 (RCA-GUESS vs. HIRHAM5-DMI) to 0.4 (RCA4 vs. RCA-GUESS) in summer (Table 2). RCA4 and RCA-GUESS show high correlations for both seasons, which is likely due to their sharing models physics. The same is found for HIRHAM-AWI and HIRHAM-DMI.

In general, the large agreement on cyclone frequency across the different RCMs using the same GCM forcing indicates the dominant impact of the GCM forcing compared to the RCM physics. However, the magnitude of changes can vary across the regional projections, which shows the imprint of internal RCM model processes.

### 5.3. Effects of empirically corrected SST

Here we assess the impact of empirical correction of SST on changes of cyclone frequency using the two CRCM5 runs: CRCM5-MPI and CRCM5-MPIC. The latter represents a run with corrected SST. The basic approach of this empirical correction is the assumption that biases in the historical simulation will persist in the future scenario projections. Therefore, the sea-surface conditions simulated by a GCM are empirically corrected by subtracting the biases identified from the historical simulations. More detailed information can be found in Takhsha et al. (2017).

Fig. 3 indicates that the overall Arctic changes of all cyclone characteristics (frequency, depth, size) are practically the same in both runs. Cyclone frequency and size are projected to increase (decrease) in winter (summer), while cyclone depth is projected to decrease in both seasons, consistently in both runs. Spatial differences in cyclone frequency changes are noted for the Beaufort and Nordic Seas and Baffin Bay in winter and for Svalbard and the Arctic Ocean in summer (Fig. 7). There is a significant decrease of cyclone frequency in the Barents Sea in the CRCM5-MPI in winter, which is absent in the CRCM5-MPIC. A strong decrease of summer cyclone frequency is also simulated by the CRCM5-MPI over the Arctic Ocean in contrast to an increase in the CRCM5-MPIC. Therefore, spatial correlation coefficients between the CRCM5-MPIC and CRCM5-MPI patterns of change are low for both seasons (Table 2).

The main reason for the differences in cyclone activity in the CRCM5-MPI and CRCM5-MPIC simulations is related to different changes of baroclinicity. There are two major factors influencing the baroclinicity and thus cyclone activity; the Brunt-Väisälä frequency, which is related to the vertical temperature gradient and is a measure of temperature stratification, and vertical wind shear, which is related to the horizontal temperature gradient. Therefore, a possible explanation of the different changes in cyclone characteristics is the difference in vertical and horizontal temperature response. The differences between the two simulations over the Barents Sea in winter can be explained by

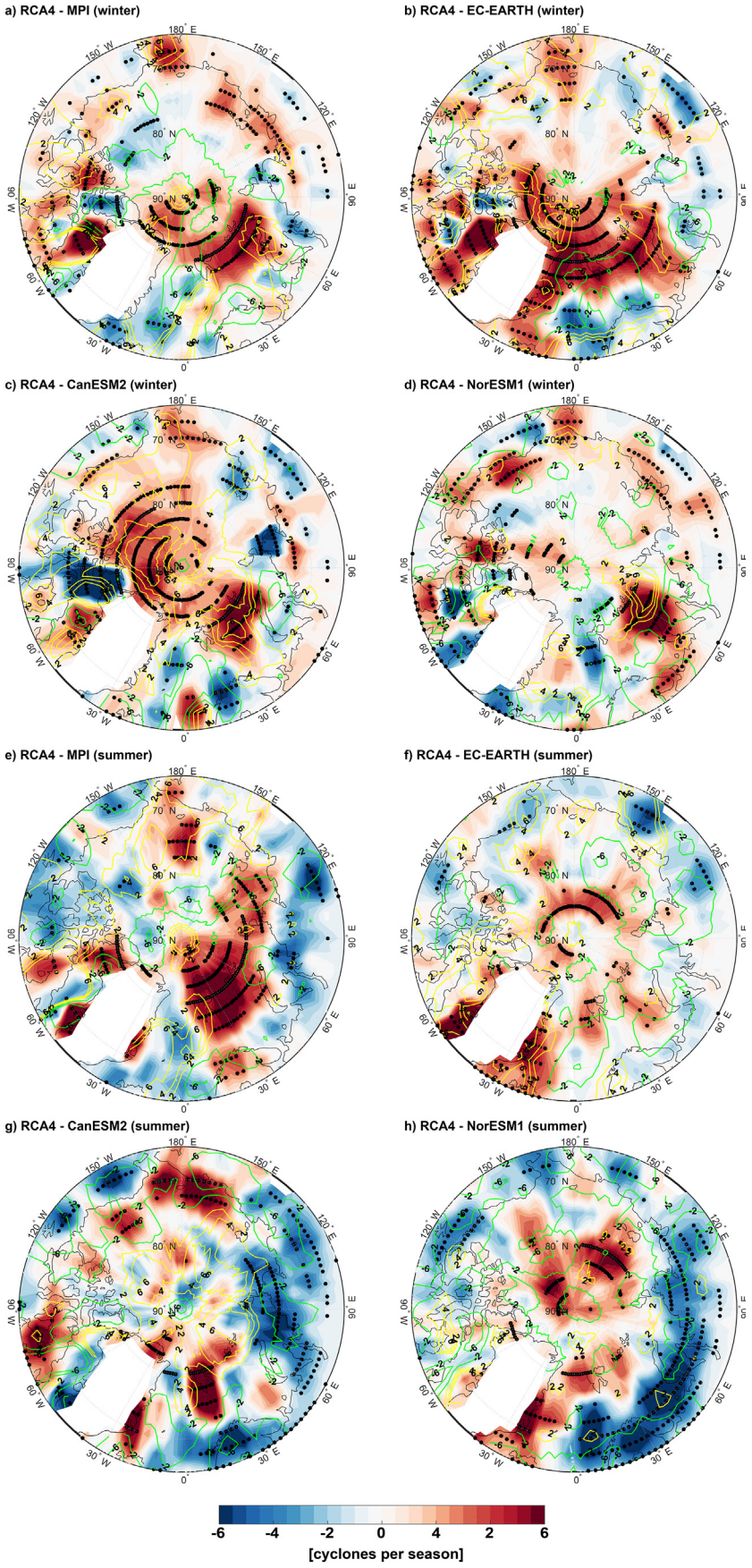


**Fig. 5.** Projected changes of cyclone frequency ("RCP8.5" – "hist") from RCA4 with different BCs for winter (a-d) and summer (e-h). Yellow (positive) and green (negative) isolines show the associated GCM changes. Black dots show statistical significance ($p < .1$) of the RCM projections. Cyclones over regions with surface elevations higher than 1000 m are masked out. (For interpretation of the references to colour in this figure legend, the reader is referred to the web version of this article.)

**Table 2**
Spatial correlation coefficients for cyclone frequency changes from RCMs and GCMs for winter/summer (colour highlights moderate and large correlation; green: $R = 0.4$, blue: $R = 0.5$, red: $R = 0.6$).

| winter/summer | MPI-ESM-LR | EC-EARTH | CanESM2 | NorESM1 | HIRHAM5-AWI-MPI | HIRHAM5-AWI-EC-EARTH | CRCM5-MPI | CRCM5-MPIC | CRCM5-CanESM2 | RCA4 -MPI | RCA4-EC-EARTH | RCA4-CanESM2 | RCA4-NorESM1 | RCA-GUESS-EC-EARTH | MAR3.6-NorESM1 | HIRHAM5-DMI-EC-EARTH |
|---|---|---|---|---|---|---|---|---|---|---|---|---|---|---|---|---|
| **HIRHAM5-AWI-MPI** | 0.3/-0.3 | 0.3/-0.2 | 0.2/0.3 | 0.1/0.2 | - | 0.3/0.1 | 0.0/0.2 | 0.3/-0.3 | 0.2/0.3 | **0.5**/-0.2 | 0.2/0.2 | **0.4**/0.2 | **0.4**/0.0 | 0.2/0.0 | 0.2/0.0 | 0.3/0.2 |
| **HIRHAM5-AWI-EC-EARTH** | 0.0/**0.4** | **0.4**/0.1 | 0.4/0.0 | 0.2/-0.2 | 0.3/0.1 | - | 0.1/-0.2 | 0.3/0.1 | 0.2/0.1 | **0.5**/0.1 | **0.5**/0.3 | 0.2/0.2 | 0.2/0.3 | **0.5**/**0.4** | 0.1/0.3 | **0.4**/0.2 |
| **CRCM5-MPI** | 0.0/0.0 | 0.1/0.1 | 0.0/-0.3 | 0.2/0.2 | 0.0/0.2 | 0.1/-0.2 | - | 0.2/0.1 | 0.2/0.3 | 0.25/0.25 | -0.2/-0.3 | -0.1/0 | 0.0/-0.4 | -0.2/-0.4 | 0.0/-0.1 | 0.2/0.0 |
| **CRCM5-MPIC** | 0.3/0.2 | **0.4**/0.2 | 0.1/-0.1 | 0.0/-0.1 | 0.3/-0.3 | 0.3/0.1 | 0.2/0.1 | - | 0.1/0.2 | **0.4**/0.1 | 0.2/0.0 | 0.2/-0.1 | 0.2/0.2 | 0.2/0.2 | 0.1/0.3 | 0.2/0.2 |
| **CRCM5-CanESM2** | 0.2/0.0 | 0.3/0.0 | 0.3/0.1 | -0.1/0.1 | 0.2/0.3 | 0.2/0.1 | 0.2/0.3 | 0.1/0.2 | - | 0.2/-0.2 | 0.3/-0.1 | **0.4**/0.2 | 0.3/0.1 | 0.3/0.0 | 0.0/0.1 | 0.2/0.3 |
| **RCA4 -MPI** | 0.2/0.2 | 0.3/0.1 | 0.3/0.0 | 0.1/-0.1 | **0.5**/-0.2 | **0.5**/0.1 | -0.1/-0.4 | **0.4**/0.1 | 0.2/-0.2 | - | **0.6**/0.4 | **0.4**/0.2 | **0.5**/**0.4** | **0.5**/**0.5** | 0.2/0.1 | **0.4**/**0.0** |
| **RCA4-EC-EARTH** | 0.1/-0.1 | 0.3/-0.1 | **0.4**/**0.4** | 0.0/0.2 | 0.2/0.2 | **0.5**/0.3 | -0.2/-0.3 | 0.2/0.0 | 0.3/-0.1 | **0.6**/**0.4** | - | **0.5**/0.3 | 0.3/**0.4** | **0.6**/**0.4** | 0.0/0.2 | **0.5**/0.2 |
| **RCA4-CanESM2** | 0.3/0.1 | 0.1/0.0 | 0.2/0.2 | 0.0/0.1 | **0.4**/0.2 | 0.2/0.2 | -0.1/0 | 0.2/-0.1 | **0.4**/0.2 | **0.4**/0.2 | **0.5**/0.3 | - | 0.3/0.2 | **0.5**/0.2 | 0.0/0.1 | 0.2/0.3 |
| **RCA4-NorESM1** | 0.2/0.3 | 0.2/0.2 | 0.1/0.1 | 0.0/-0.2 | **0.4**/0.0 | 0.2/0.3 | 0.0/-0.4 | 0.2/0.2 | 0.3/0.1 | **0.5**/**0.4** | 0.3/**0.4** | 0.3/0.2 | - | 0.3/**0.4** | **0.4**/**0.4** | 0.2/0.2 |
| **RCA-GUESS-EC-EARTH** | 0.0/0.2 | 0.2/0.0 | **0.4**/0.1 | 0.0/0.0 | 0.2/0.0 | **0.5**/**0.4** | **0.5**/**0.5** | 0.2/0.2 | 0.3/0.0 | **0.5**/**0.5** | **0.6**/**0.4** | **0.5**/0.2 | 0.3/**0.4** | - | 0.0/0.2 | 0.3/0.1 |
| **MAR3.6-NorESM1** | 0.1/0.2 | 0.3/0.3 | 0.0/0.0 | 0.1/0.1 | 0.2/0.0 | 0.1/0.3 | 0.0/-0.1 | 0.1/0.3 | 0.0/0.1 | 0.2/0.1 | 0.0/0.2 | 0.0/0.1 | **0.4**/**0.4** | 0.0/0.2 | - | 0.0/0.2 |
| **HIRHAM5-DMI-EC-EARTH** | 0.0/-0.2 | **0.4**/-0.1 | **0.5**/**0.4** | 0.2/0.2 | 0.3/0.2 | **0.4**/0.2 | 0.2/0.0 | 0.2/0.2 | 0.2/0.3 | **0.4**/0.0 | **0.5**/0.2 | 0.2/0.3 | 0.2/0.2 | 0.3/0.1 | 0.0/0.2 | - |

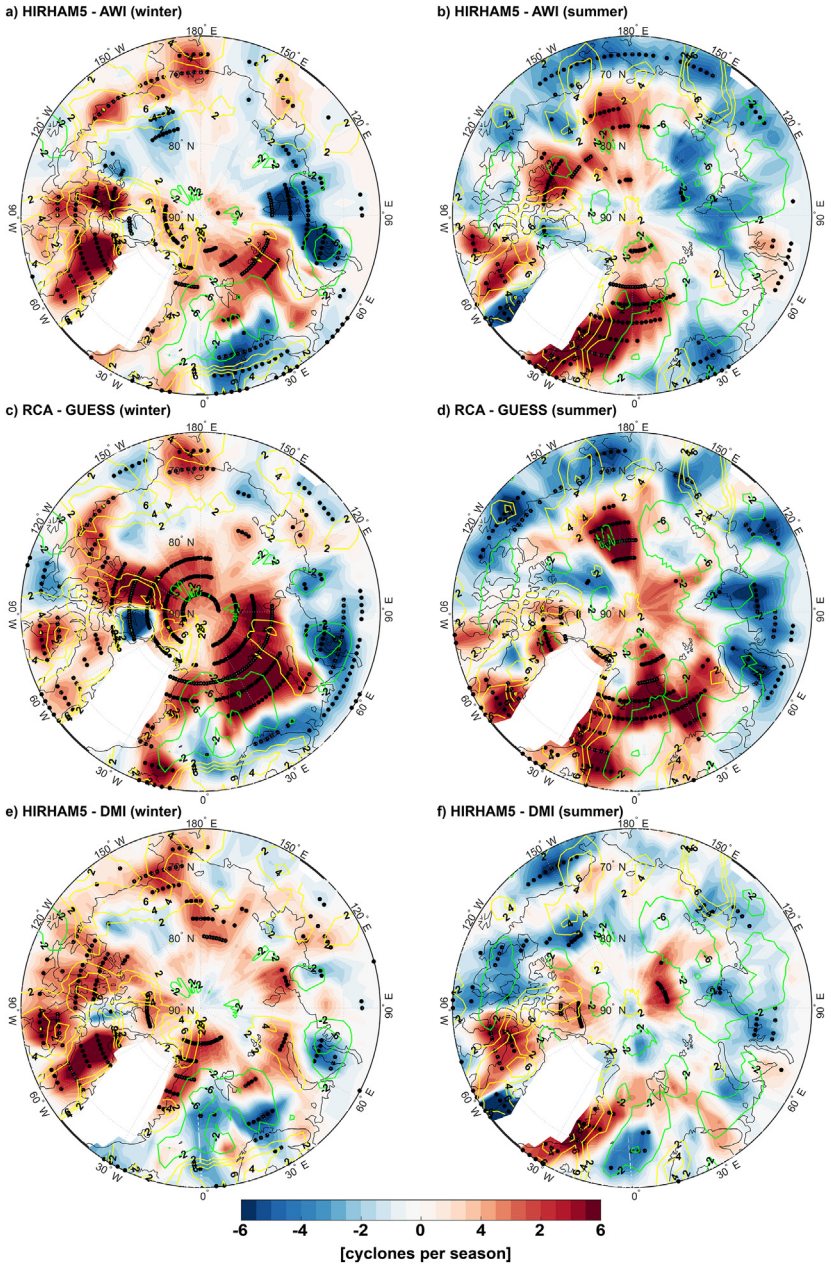


**Fig. 6.** Projected changes of cyclone frequency ("RCP8.5" – "hist") from EC-EARTH driven models for winter (a,c,e) and summer (b,d,f). The associated results for RCA4 are shown in Fig. 5. Yellow (positive) and green (negative) isolines show the associated GCM changes. Black dots show statistical significance ($p < .1$) of the RCM projections. Cyclones over regions with surface elevations higher than 1000 m are masked out. (For interpretation of the references to colour in this figure legend, the reader is referred to the web version of this article.)

different changes in vertical static stability. For this, we show the difference between sea surface temperature and air temperature at 500 hPa (Supplementary Fig. 7), which is a commonly used measure of static stability and polar mesocyclone activity in the Arctic (e.g. Zahn and Von Storch, 2008). Differences in vertical static stability changes between CRCM5-MPI and CRCM5-MPIC runs become obvious for the Barents Seas in winter, leading also to different changes of mesocyclone activity (Mokhov et al., 2007). In summer, changes in cyclone frequency over the Arctic Ocean can be explained by a strong contrast between the warming over the Arctic Ocean and over the continents in CRCM5-MPIC, compared to CRCM5-MPI (Supplementary Fig. 8). Related with this, Serreze and Barrett (2008) showed that the summer maximum in cyclone activity over the Arctic Ocean centered near the North Pole is associated with cyclones generated over the Eurasian continent.

## 6. Summary and conclusion

We analyzed possible future changes of cyclone characteristics (frequency, depth, and size) over the Arctic using the largest existing ensemble of RCM simulations (Arctic-CORDEX) for the 21st century based on the RCP8.5 scenario. Changes of cyclone characteristics from RCMs have been compared with four GCMs, which have been used as boundary condition for the RCM projections.

The similarity of changes of cyclone characteristics in RCMs and corresponding GCMs depends strongly on the region and season. Both, the RCMs and GCMs consistently show an increase of cyclone frequency over the Baffin Bay, Barents Sea, north of Greenland, Canadian Archipelago, and a decrease over the Nordic Seas, Kara and Beaufort Seas and over the sub-arctic continental areas in winter. In summer, the frequency increases over some parts of the Arctic Ocean and Greenland

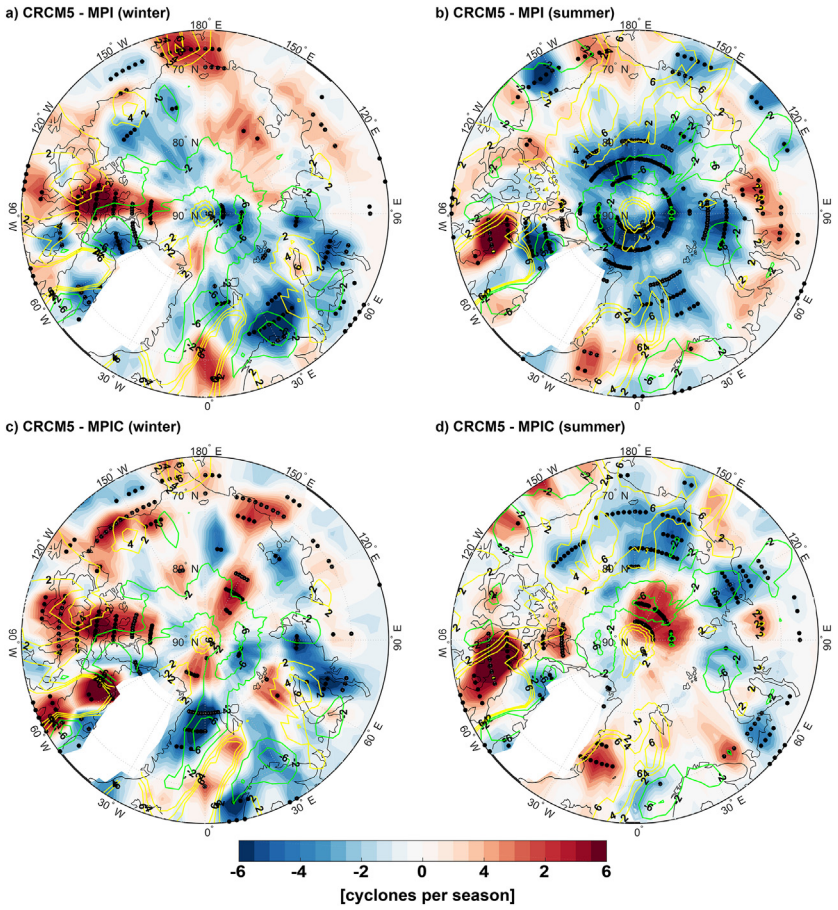


**Fig. 7.** Projected changes of cyclone frequency ("RCP8.5" – "hist") from CRCM5 with MPI-ESM-LR forcing with (MPIC) and without (MPI) SST correction for winter (a,c) and summer (b,d).). Yellow (positive) and green (negative) isolines show the associated GCM changes. Black dots show statistical significance ($p < .1$) of the RCM projections. Cyclones over regions with surface elevations higher than 1000 m are masked out. (For interpretation of the references to colour in this figure legend, the reader is referred to the web version of this article.)

Sea and decreases over the Norwegian and Kara Seas and over the continents, in particular, over east Siberia and Alaska. Differences in changes of cyclone frequency between RCMs and GCMs are found in winter over the Arctic Ocean, where most of the RCMs show an increase, whereas the GCMs show a consistent decrease. Most RCMs also simulate a decrease over the East Siberian Sea, whereas the GCMs show an increase. In summer, differences are also obvious for most parts of the Arctic Ocean, where most RCMs show positive changes, whereas most GCMs exhibit negative changes in cyclone frequency.

We also assessed the influence of the GCM boundary conditions and RCM physics on the projected cyclone characteristics changes. In general, the GCM boundary forcing is more important than RCM physics, particularly in winter. However, the magnitude of changes can vary across the RCMs, which shows the imprint of internal RCM model processes. This is noticeable, because the majority of Arctic cyclones form within the Arctic basin (Sepp and Jaagus, 2011). But the conclusion is in line with previous RCM studies over Europe (e.g. Frei et al., 2006; Déqué et al., 2012; Beniston et al., 2007; Christensen and Christensen, 2007; Koenigk et al., 2015; Colmet-Daage et al., 2018), which concluded that for most seasons and for most regions, the choice of GCM has a larger effect for the simulated seasonal temperature changes than the choice of RCM. The significant role of the SST forcing for the projected temperature and changes of cyclone activity in the Arctic, in particular over the Nordic Seas and Arctic Ocean, was revealed in our study when comparing runs with and without SST correction. Cyclone frequency changes are different in these runs: a reduction in both summer and winter in CRCM5-MPI but an increase in winter and small change in summer in CRCM5-MPIC. These differences were related to a different representation of vertical and horizontal temperature distributions, which may significantly change the stability in the atmosphere and thus cyclone characteristics and their changes in the Arctic.

The given results for Arctic cyclone changes at the end of the 21st century under the RCP8.5 scenario are based on a small-sized RCM-GCM matrix including 12 RCM simulations driven by four GCMs, which imposes a limitation on the climate change signal robustness. Thus, it is important that upcoming regional model experiments comprise larger ensembles to better separate the forced signal from natural variability.

## Acknowledgements

M.A., I.I.M., V.A.S., A.R., K.D. acknowledge the support by the project "Quantifying Rapid Climate Change in the Arctic: regional feedbacks and large-scale impacts (QUARCCS)" funded by the German and Russian Ministries of Research and Education. V.A.S. was supported by the Russian Science Foundation (RSF № 19-17-00242). M.A, I.I.M, and M.A.D. were supported by the projects funded by RFBR (№ 17-05-01097, 18-05-60216, 18-35-00091). A.R. and K.D. acknowledge the funding by the Deutsche Forschungsgemeinschaft (DFG, German Research Foundation) – Project number 268020496 – TRR 172, within the Transregional Collaborative Research Center "ArctiC Amplification: Climate Relevant Atmospheric and SurfaCe Processes, and Feedback Mechanisms (AC)$^3$". T. K. acknowledges the support by the NordForsk-funded Nordic Centre of Excellence project (award 76654) Arctic Climate Predictions: Pathways to Resilient, Sustainable Societies (ARCPATH). D.S. was supported by the PRIMAVERA project, which has received funding from the European Union's Horizon 2020 research and innovation programme under grant agreement No 641727 and the state assignment (theme 0149-2019-0015). We acknowledge the Japan Meteorological Agency (JMA) for providing JRA-55, the European Centre for Medium- Range Weather Forecasts (ECMWF) for providing ERA-Interim, the National Centers for Environmental Prediction

(NCEP) for providing NCEP-CFSR, NASA Goddard Earth Sciences (GES) Data and Information Services Center (DISC) for providing MERRA2. Data from reanalyses were retrieved from https://reanalyses.org/atmosphere/overview-current-atmospheric-reanalyses/. The data that support the findings of this study are available from the corresponding author upon reasonable request. Finally, we thank two anonymous reviewers for their valuable comments on this manuscript.

## Appendix A. Supplementary data

Supplementary data to this article can be found online at https://doi.org/10.1016/j.gloplacha.2019.103005.

## References

Akperov, M.G., Mokhov, I.I., 2010. A comparative analysis of the method of extratropical cyclone identification. Izv. - Atmos. Ocean Phys. 46 (5). https://doi.org/10.1134/S0001433810050038.

Akperov, M.G., Mokhov, I.I., 2013. Estimates of the sensitivity of cyclonic activity in the troposphere of extratropical latitudes to changes in the temperature regime. Izv. Atmos. Ocean. Phys. 49 (2), 113–120. https://doi.org/10.1134/S0001433813020035.

Akperov, M.G., Bardin, M.Y., Volodin, E.M., Golitsyn, G.S., Mokhov, I.I., 2007. Probability distributions for cyclones and anticyclones from the NCEP/NCAR reanalysis data and the INM RAS climate model. Izv. Atmos. Ocean. Phys. 43 (6), 705–712. https://doi.org/10.1134/S0001433807060047.

Akperov, M., Mokhov, I., Rinke, A., Dethloff, K., Matthes, H., 2015. Cyclones and their possible changes in the Arctic by the end of the twenty first century from regional climate model simulations. Theor. Appl. Climatol. 122 (1–2), 85–96. https://doi.org/10.1007/s00704-014-1272-2.

Akperov, M., et al., 2018. Cyclone activity in the Arctic from an ensemble of regional climate models (Arctic CORDEX). J. Geophys. Res. Atmos. https://doi.org/10.1002/2017JD027703.

Alexeev, V.A., Walsh, J.E., Ivanov, V.V., Semenov, V.A., Smirnov, A.V., 2017. Warming in the Nordic Seas, North Atlantic storms and thinning Arctic sea ice. Environ. Res. Lett. 12 (8). https://doi.org/10.1088/1748-9326/aa7a1d.

Arora, V., Scinocca, J., Boer, G., Christian, J., Denman, K., Flato, G., Kharin, V., Lee, W., Merryfield, W., 2011. Carbon emission limits required to satisfy future representative concentration pathways of green- house gases. Geophys. Res. Lett. 38 (5) (doi: 0.1029/2010GL046270).

Bardin, M.Y., Polonsky, A.B., 2005. North Atlantic oscillation and synoptic variability in the European- Atlantic region in winter. Izv. Atmos. Ocean. Phys. 41 (April), 127–136.

Beniston, M., et al., 2007. Future extreme events in European climate: an exploration of regional climate model projections. Clim. Chang. 81, 71–95. https://doi.org/10.1007/s10584-006-9226-z. SUPPL. 1.

Bentsen, M., et al., 2013. The Norwegian Earth System Model, NorESM1-M – part 1: description and basic evaluation of the physical climate. Geosci. Model Dev. 6 (3), 687–720. https://doi.org/10.5194/gmd-6-687-2013.

Berg, P., Döscher, R., Koenigk, T., 2013. Impacts of using spectral nudging on regional climate model RCA4 simulations of the Arctic. Geosci. Model Dev. 6 (3), 849–859. https://doi.org/10.5194/gmd-6-849-2013.

Christensen, J.H., Christensen, O.B., 2007. A summary of the PRUDENCE model projections of changes in European climate by the end of this century. Clim. Chang. 81, 7–30. https://doi.org/10.1007/s10584-006-9210-7. SUPPL. 1.

Christensen, O.B., Drews, M., Christensen, J.H., Dethloff, K., Ketelsen, K., Hebestadt, I., Rinke, A., 2007. *DMI Technical report,* 06–17. In: The HIRHAM Regional Climate Model Version 5 (β).

Colle, B.A., Zhang, Z., Lombardo, K.A., Chang, E., Liu, P., Zhang, M., 2013. Historical evaluation and future prediction of Eastern North American and Western Atlantic Extratropical Cyclones in the CMIP5 models during the cool season. J.Climate 26, 6882–6903. https://doi.org/10.1175/JCLI-D-12-00498.1.

Colmet-Daage, A., Sanchez-Gomez, E., Ricci, S., Llovel, C., Estupina, V.B., Quintana-Seguí, P., Carmen Llasat, M., Servat, E., 2018. Evaluation of uncertainties in mean and extreme precipitation under climate change for northwestern Mediterranean watersheds from high-resolution Med and Euro-CORDEX ensembles. Hydrol. Earth Syst. Sci. 22 (1), 673–687. https://doi.org/10.5194/hess-22-673-2018.

Côté, H., Grise, K.M., Son, S.W., de Elía, R., Frigon, A., 2015. Challenges of tracking extratropical cyclones in regional climate models. Clim. Dyn. 44 (11 − 12), 3101–3109. https://doi.org/10.1007/s00382-014-2327-x.

Crawford, A.D., Serreze, M.C., 2017. Projected changes in the arctic frontal zone and summer arctic cyclone activity in the CESM large ensemble. J. Clim. 30 (24), 9847–9869. https://doi.org/10.1175/JCLI-D-17-0296.1.

Day, J.J., Hodges, K.I., 2018. Growing land-sea temperature contrast and the intensification of Arctic cyclones. Geophys. Res. Lett. 3673–3681. https://doi.org/10.1029/2018GL077587.

Dee, D.P., et al., 2011. The ERA-Interim reanalysis: configuration and performance of the data assimilation system. Q. J. R. Meteorol. Soc. 137 (656), 553–597. https://doi.org/10.1002/qj.828.

Déqué, M., Somot, S., Sanchez-Gomez, E., Goodess, C.M., Jacob, D., Lenderink, G., Christensen, O.B., 2012. The spread amongst ENSEMBLES regional scenarios: regional climate models, driving general circulation models and interannual variability. Clim. Dyn. 38 (5–6), 951–964. https://doi.org/10.1007/s00382-011-1053-x.

Ebita, A., et al., 2011. The Japanese 55-year reanalysis "JRA-55": an interim report. SOLA 7, 149–152.

Fettweis, X., Box, J.E., Agosta, C., Amory, C., Kittel, C., Lang, C., van As, D., Machguth, H., Gallee, H., 2017. Reconstructions of the 1900–2015 Greenland ice sheet surface mass balance using the regional climate MAR model. Cryosph. 11, 1015–1033. https://doi.org/10.5194/tc-11-1015-2017.

Frei, C., Schöll, R., Fukutome, S., Schmidli, J., Vidale, P.L., 2006. Future change of precipitation extremes in Europe: Intercomparison of scenarios from regional climate models. J. Geophys. Res. Atmos. 111 (6). https://doi.org/10.1029/2005JD005965.

Gelaro, R., et al., 2017. The modern-era retrospective analysis for research and applications, Version 2 (MERRA-2). J. Clim. 30, 5419–5454.

Giorgetta, M.A., et al., 2013. Climate and carbon cycle changes from 1850 to 2100 in MPI-ESM simulations for the coupled Model Intercomparison Project phase 5. J. Adv. Model. Earth Syst. 5 (3), 572–597. https://doi.org/10.1002/jame.20038.

Giorgi, F., Jones, C., Asrar, G., 2009. Addressing climate information needs at the regional level: the CORDEX framework. WMO Bull 175–183.

Golitsyn, G.S., Mokhov, I.I., Akperov, M.G., Bardin, M.Y., 2007. Distribution functions of probabilities of cyclones and anticyclones from 1952 to 2000: an instrument for the determination of global climate variations. Dokl. Earth Sci. 413 (1), 324–326. https://doi.org/10.1134/S1028334X07020432.

Harvey, B.J., Shaffrey, L.C., Woollings, T.J., 2015. Deconstructing the climate change response of the Northern Hemisphere wintertime storm tracks. Clim. Dyn. 45 (9–10), 2847–2860. https://doi.org/10.1007/s00382-015-2510-8.

Hazeleger, W., et al., 2012. EC-Earth: a seamless Earth-system prediction approach in action. Clim. Dyn. 39 (11), 2609–2610. https://doi.org/10.1175/2010BAMS2877.1.

Inoue, J., Hori, M.E., Takaya, K., 2012. The role of barents sea ice in the wintertime cyclone track and emergence of a warm-arctic cold-Siberian anomaly. J. Clim. 25 (7), 2561–2568. https://doi.org/10.1175/JCLI-D-11-00449.1.

Khon, V.C., Mokhov, I.I., Semenov, V.A., 2017. Transit navigation through Northern Sea Route from satellite data and CMIP5 simulations. Environ. Res. Lett. 7 (12), 024010. https://doi.org/10.1088/1748-9326/aa5841.

Klaus, D., Dethloff, K., Dorn, W., Rinke, A., Wu, D.L., 2016. New insight of Arctic cloud parameterization from regional climate model simulations, satellite-based, and drifting station data. Geophys. Res. Lett. 43, 5450–5459. https://doi.org/10.1002/2015GL067530.

Kobayashi, S., Ota, Y., Harada, Y., Ebita, A., Moriya, M., Onoda, H., Onogi, K., Kamahori, H., Kobayashi, C., Endo, H., Miyaoka, K., Takahashi, K., 2015. The JRA-55 reanalysis: general specifications and basic characteristics. J. Meteorol. Soc. Japan 93, 5–48. https://doi.org/10.2151/jmsj.2015-001.

Koenigk, T., P. Berg, and R. Döscher (2015), Arctic climate change in an ensemble of regional CORDEX simulations, Polar Res., 34, 1–19, doi:https://doi.org/10.3402/polar.v34.24603.

Lang, C., Waugh, D.W., 2011. Impact of climate change on the frequency of Northern Hemisphere summer cyclones. J. Geophys. Res. Atmos. 116 (4), 1–12. https://doi.org/10.1029/2010JD014300.

Lee, R.W., 2014. Storm Track Biases and Changes in a Warming Climate from an Extratropical Cyclone Perspective Using CMIP5. PhD Thesis. University of Reading.

Lucas-Picher, P., Wulff-Nielsen, M., Christensen, J.H., Aðalgeirsdóttir, G., Mottram, R., Simonsen, S.B., 2012. Very high resolution regional climate model simulations over Greenland: Identifying added value. J. Geophys. Res. Atmos. 117, D02108. https://doi.org/10.1029/2011JD016267.

Martynov, A., Laprise, R., Sushama, L., Winger, K., Šeparović, L., Dugas, B., 2013. Reanalysis-driven climate simulation over CORDEX North America domain using the Canadian Regional climate Model, version 5: model performance evaluation. Clim. Dyn. 41, 2973–3005. https://doi.org/10.1007/s00382-013-1778-9.

Mba, W.P., et al., 2018. Consequences of 1.5 °c and 2 °c global warming levels for temperature and precipitation changes over Central Africa. Environ. Res. Lett. 13 (5). https://doi.org/10.1088/1748-9326/aab048.

Mokhov, I.I., Mokhov, O.I., Petukhov, V.K., Khayrullin, R.R., 1992. Effect of global climatic changes on the cyclonic activity in the atmosphere. Izv. Atmos. Ocean. Phys. 28 (1), 7–18.

Mokhov, I.I., Akperov, M.G., Lagun, V.E., Lutsenko, E.I., 2007. Intense Arctic mesocyclones. Izv. Atmos. Ocean. Phys. 43, 259–265. https://doi.org/10.1134/S0001433807030012.

Neu, U., et al., 2013. Imilast: a community effort to intercompare extratropical cyclone detection and tracking algorithms. Bull. Am. Meteorol. Soc. 94 (4). https://doi.org/10.1175/BAMS-D-11-00154.1.

Nikulin, G., et al., 2018. The effects of 1.5 and 2 degrees of global warming on Africa in the CORDEX ensemble. Environ. Res. Lett. 13 (6). https://doi.org/10.1088/1748-9326/aab1b1.

Nishii, K., Nakamura, H., Orsolini, Y.J., 2015. Arctic summer storm track in CMIP3/5 climate models. Clim. Dyn. 44 (5–6), 1311–1327. https://doi.org/10.1007/s00382-014-2229-y.

Orsolini, Y.J., Sorteberg, A., 2009. Projected changes in eurasian and arctic summer cyclones under global warming in the bergen climate model. Atmos. Ocean. Sci. Lett. 2 (1), 62–67. https://doi.org/10.1080/16742834.2009.11446776.

Saha, Suranjana, et al., 2010. The NCEP Climate Forecast System Reanalysis. Bull. Amer. Meteor. Soc. 91, 1015–1057. https://doi.org/10.1175/2010BAMS3001.1.

Semenov, V.A., Latif, M., 2015. Nonlinear winter atmospheric circulation response to Arctic sea ice concentration anomalies for different periods during 1966–2012. Environ. Res. Lett. 10, 054020. https://doi.org/10.1088/1748-9326/10/5/054020.

Šeparović, L., Alexandru, A., Laprise, R., Martynov, A., Sushama, L., Winger, K., Tete, K., Valin, M., 2013. Present climate and climate change over North America as simulated by the fifth-generation Canadian regional climate model. Clim. Dyn. 41, 3167–3201.

https://doi.org/10.1007/s00382-013-1737-5.
Sepp, M., Jaagus, 2011. Changes in the activity and tracks of Arctic cyclones, Clim. Change 105, 577. https://doi.org/10.1007/s10584-010-9893-7.
Serreze, M.C., Barrett, A.P., 2008. The summer cyclone maximum over the central Arctic Ocean. J. Clim. 21, 1048–1065. https://doi.org/10.1175/2007JCLI1810.1.
Shkolnik, I.M., Efimov, S.V., 2013. Cyclonic activity in high latitudes as simulated by a regional atmospheric climate model: added value and uncertainties. Environ. Res. Lett. 8 (4), 045007. https://doi.org/10.1088/1748-9326/8/4/045007.
Simmonds, I., Keay, K., 2009. Extraordinary September Arctic sea ice reductions and their relationships with storm behavior over 1979-2008. Geophys. Res. Lett. 36, 19), 1–5. https://doi.org/10.1029/2009GL039810.
Simmonds, I., Rudeva, I., 2014. A comparison of tracking methods for extreme cyclones in the Arctic basin. Tellus A 1 (August), 1–13. https://doi.org/10.3402/tellusa.v66.25252.
Simmonds, I., Burke, C., Keay, K., 2008. Arctic climate change as manifest in cyclone behavior. J. Clim. 21 (22), 5777–5796. https://doi.org/10.1175/2008JCLI2366.1.
Smith, B., Samuelsson, P., Wramneby, A., Rummukainen, M., 2011. A model of the coupled dynamics of climate, vegetation and terrestrial ecosystem biogeochemistry for regional applications. Tellus Ser. A Dyn. Meteorol. Oceanogr. 63 (1), 87–106. https://doi.org/10.1111/j.1600-0870.2010.00477.x.
Sommerfeld, A., Nikiema, O., Rinke, A., Dethloff, K., Laprise, R., 2015. Arctic budget study of intermember variability using HIRHAM5 ensemble simulations. J. Geophys. Res. Atmos. 120, 9390–9407. https://doi.org/10.1002/2015JD023153.
Takhsha, M., Nikiéma, O., Lucas-Picher, P., Laprise, R., Hernández-Díaz, L., Winger, K., 2017. Dynamical downscaling with the fifth-generation Canadian regional climate model (CRCM5) over the CORDEX Arctic domain: effect of large-scale spectral nudging and of empirical correction of sea-surface temperature. Clim. Dyn. 0, 1–26. https://doi.org/10.1007/s00382-017-3912-6. (0).
Taylor, K.E., Stouffer, R.J., Meehl, G.A., 2012. An overview of CMIP5 and the experiment design. Bull. Am. Meteorol. Soc. 93, 485–498. https://doi.org/10.1175/BAMS-D-11-00094.1.
Ulbrich, U., et al., 2013. Are Greenhouse Gas Signals of Northern Hemisphere winter extra-tropical cyclone activity dependent on the identification and tracking algorithm? Meteorol. Z. 22 (1). https://doi.org/10.1127/0941-2948/2013/0420.
Vihma, T., 2014. Effects of Arctic Sea Ice Decline on Weather and Climate: A Review. Surv. Geophys. https://doi.org/10.1007/s10712-014-9284-0.
Wernli, H., Schwierz, C., 2006. Surface cyclones in the ERA-40 dataset (1958–2001). Part I: Novel identification method and global climatology. J. Atmos. Sci. 63, 2486–2507. https://doi.org/10.1175/JAS3766.1.
Zahn, M., Von Storch, H., 2008. A long-term climatology of North Atlantic polar lows. Geophys. Res. Lett. 35 (22), 1–6. https://doi.org/10.1029/2008GL035769.
Zahn, M., Akperov, M., Rinke, A., Feser, F., Mokhov, I.I., 2018. Trends of cyclone characteristics in the arctic and their patterns from different reanalysis data. J. Geophys. Res. Atmos. https://doi.org/10.1002/2017JD027439.
Zappa, G., Shaffrey, L.C., Hodges, K.I., 2013. The ability of CMIP5 models to simulate North Atlantic extratropical cyclones. J. Clim. 26 (15), 5379–5396. https://doi.org/10.1175/JCLI-D-12-00501.1.
Zhang, W., Jansson, C., Miller, P.A., Smith, B., Samuelsson, P., 2014. Biogeophysical feedbacks enhance the arctic terrestrial carbon sink in regional earth system dynamics. Biogeosciences 11 (19), 5503–5519. https://doi.org/10.5194/bg-11-5503-2014.